Internal Report
DESY M 97-06
June 1997

Design of a High Power Standing Wave Test Resonator for SBLC Cells

V. E. Kaljuzhny, S. N. Yarigin

Moscow Engineering Physics Institute MEPhI, Moscow, Russia

M. Dohlus, N. Holtkamp, S. Wipf

Deutsches Elektronen-Synchrotron DESY, Hamburg, Germany

1. Introduction

A test device has already been manufactured for the investigations of the properties of the iris coating, which was used for the SBLC-cups properties at high power [1]. It consisted of a 2-cell resonator and fed by a Rectangular WaveGuide which supplies the power through two slots in the wide wall of the RWG. Its construction has some disadvantages:

- cups cannot be tested at the operational frequency;
- the clystron has to be tuned to another frequency, therefore the maximal input power is not available.
- the procedure for exchanging cups is rather complicated, because it requires an indium wire to be manually inserted into the contact slit between the cups to obtain a good vacuum properties of the structure.
- the peak field in the slot area is unknown: estimated in this work (Chapter 2.3).

The decision to design a new test machine was adopted. Requirements for it are:

- a 3 cell-resonator - to work at $2\pi/3$ standing wave mode;
- the test device should be capable of handling the field strength which corresponds to SBLC cavity operation with a SLED-system;
- additional vacuum envelope to facilitate the exchange of the test cup.

This work was started in 09.1996 and is still continuing. During this time several different models of the test device were proposed. Some of them were rejected because they were too expensive to manufacture. All of them will be described below in chronological sequence.They differ only in the design of the power input into 3-cell standing wave resonators in which the central cup is the test one.

2. Coupling of a resonator to a waveguide by inductive slots

In this chapter the coupling method which was used for the original test device will be considered by means of a mathematical model.

2.1 Two resonators coupled through a narrow slot.

Let us consider two resonant cavities coupled by magnetic field through a narrow slot, see Figure 1

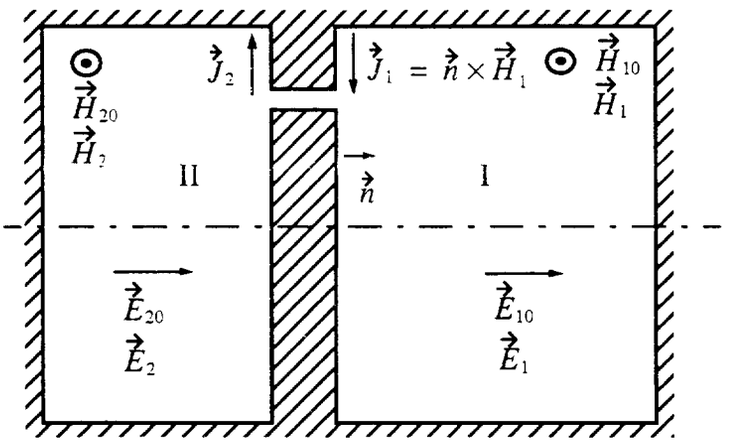

Figure 1: Two cylindrical resonators coupled through the slot.

Maxwell equations for cavity I without slots is:

$$\begin{cases} \mathrm{curl}\vec{E}_{10} = -j\omega_0\mu_0\vec{H}_{10} \\ \mathrm{curl}\vec{H}_{10} = j\omega_0\mu_0\vec{E}_{10} \\ \vec{n}\cdot\vec{H}_{10} = 0 \\ \vec{n}\times\vec{E}_{10} = 0 \end{cases} \tag{1}$$

The same equations can be written for the case with a slot, except for the boundary conditions:

$$\begin{cases} \mathrm{curl}\vec{E}_1 = -j\omega\mu_0\vec{H}_1 \\ \mathrm{curl}\vec{H}_1 = j\omega\varepsilon_0\vec{E}_1 \\ \left.\begin{aligned} \vec{n}\cdot\vec{H}_1 = 0 \\ \vec{n}\times\vec{E}_1 = 0 \end{aligned}\right\} & \text{on the cavity surface} \\ \vec{n}\times\vec{E}_1 \neq 0 & \text{at the slot} \end{cases} \tag{2}$$

Energy stored in a cavity without a slot is defined by:

$$\int_V \varepsilon_0 E_{10}^2 dV = \int_V \mu_0 H_{10}^2 dV = 2W_{10} \tag{3}$$

For the whole volume, except for the region nearest to the slot, we assume that:

$$\vec{E}_1 = A\vec{E}_{10} \quad \text{and} \quad \vec{H}_1 = B\vec{H}_{10} \tag{4}$$

The coefficients A and B can be found from the combination of the equations written above:

$$\begin{cases} \mathrm{curl}\vec{E}_1\cdot\vec{H}_{10}^* - \mathrm{curl}\vec{H}_{10}^*\cdot\vec{E}_1 = \vec{E}_1\times\vec{H}_{10}^* = j\omega_0\varepsilon_0 E_{10}^2 A - j\omega\mu_0 H_{10}^2 B \\ \mathrm{curl}\vec{H}_1\cdot\vec{E}_{10}^* - \mathrm{curl}\vec{E}_{10}^*\cdot\vec{H}_1 = \vec{H}_1\times\vec{E}_{10}^* = j\omega\varepsilon_0 E_{10}^2 A - j\omega_0\mu_0 H_{10}^2 B \end{cases} \tag{5}$$

From the boundary conditions:

$$\begin{cases} \int_V \vec{E}_1\times\vec{H}_{10}^* dV = j\omega_0 2W_{10}A - j\omega 2W_{10}B \\ j\omega 2W_{10}A - j\omega_0 2W_{10}B = 0 \end{cases} \qquad B = \frac{\omega}{\omega_0}A \tag{6}$$

Finally:

$$\begin{aligned} B_1 &= j\frac{\omega}{\omega^2-\omega_0^2}\cdot\frac{1}{2W_{10}}\cdot\int_{S_{slot}}(\vec{E}_1\times\vec{H}_{10}^*)d\vec{S} \\ A_1 &= j\frac{\omega_0}{\omega^2-\omega_0^2}\cdot\frac{1}{2W_{10}}\cdot\int_{S_{slot}}(\vec{E}_1\times\vec{H}_{10}^*)d\vec{S} \end{aligned} \tag{7}$$

The same coefficients can be written for cell 2.

Let us consider the slot itself, in order to find the field there and to calculate

$$\int_{S_{slot}} (\vec{E}_1 \times \vec{H}_{10}^{*}) d\vec{S}, \tag{8}$$

we introduce normalised magnetic field value:

$$H_{1N} = \frac{H_{10}}{\sqrt{W}_{10}}, H_{2N} = \frac{H_{20}}{\sqrt{W}_{20}}. \tag{9}$$

The Narrow slot can be treated as a transmission line shortened at the ends. Equations for the

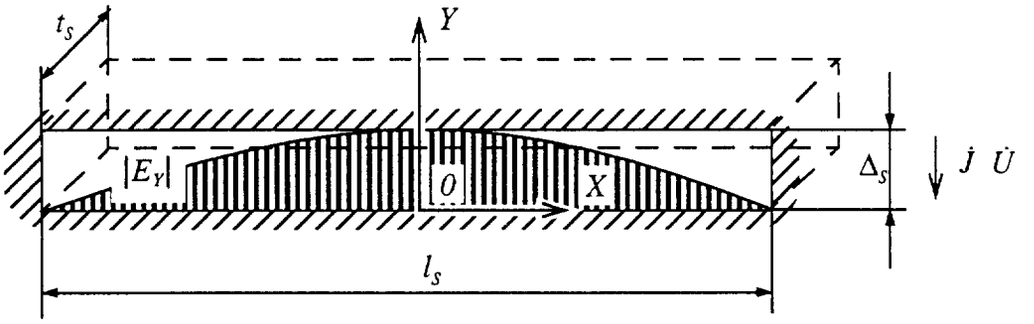

Figure 2: Electric field distribution in a slot cross-section

complex amplitudes of current $\dot{I}$ and voltage $\dot{U}$ can be written with C_0 and L_0 as the capacitance and inductance of the unit length of line ($\dot{J}$ is a surface density of a current):

$$\begin{cases} \dfrac{\partial \dot{U}}{\partial x} = -j\omega L_0 \dot{I} \\ \dfrac{\partial \dot{I}}{\partial x} = -j\omega C_0 \dot{U} + \dot{J} \end{cases} \tag{10}$$

From these equations and boundary conditions we have:

$$\dot{E}_Y(x) = \frac{\dot{U}(x)}{\Delta_s} = j\frac{1}{\omega C_0}\dot{J}\left[\frac{\cos(kx)}{\sin\left(k\frac{l}{2}\right)} - 1\right] \tag{11}$$

$$k = \omega\sqrt{L_0 C_0} = \frac{\omega}{C_0} \qquad Z_s = \sqrt{\frac{L_0}{C_0}}$$

The surface density of the current flowing through the slot is defined as

$$\dot{J} = B_1 \dot{H}_{10} - B_2 \dot{H}_{20} \tag{12}$$

and the impedance of the transmission line is (13) in accordance with [3].

$$Z_s = \sqrt{\frac{\mu_0}{\varepsilon_0}}\left[\frac{t_s}{\Delta_s} + \frac{2}{\pi}\left(1 + \ln\left(\frac{\pi t_s}{\Delta_s} + 1\right)\right)\right]^{-1} \tag{13}$$

Integral () can be calculated from (11) and multiplied by N for the case of N identical slots.

The result is a system of equations:

$$\begin{cases} \mu_0 c^2 Z_s \frac{N}{2} l \left(1 - \frac{\operatorname{tg}\left(\frac{\omega l}{2c}\right)}{\frac{\omega l}{2c}} \right) (H_{1N}^2 - A H_{1N} H_{2N}) = \omega^2 - \omega_{10}^2 \\ \mu_0 c^2 Z_s \frac{N}{2} l \left(1 - \frac{\operatorname{tg}\left(\frac{\omega l}{2c}\right)}{\frac{\omega l}{2c}} \right) \left(H_{2N}^2 - \frac{1}{A} H_{1N} H_{2N} \right) = \omega^2 - \omega_{20}^2 \end{cases} \qquad A = \frac{(\vec{H}_2 \vec{e}_Y)}{(\vec{H}_1 \vec{e}_Y)} \tag{14}$$

From this system the frequencies ω and corresponding field relation A can be found. As a result we obtain a resonant frequencies of the system which consists of two coupled resonators.

2.2 Model with power input through the narrow slots directly from the RWG.

First the most simplest model was considered which is identical to the previously used test device except for the number of cells in the standing wave resonator.

The method described in the article by Kroll and Yu [2] was used to find *Qext* of the system during the optimization of the slot dimensions. The phase-frequency pairs were calculated for the resonance model which consists of a 3-cell resonator and part of a RWG with a short circuit wall at one end (at a quarter wave length from the position of the slot) and a short circuit plunger on the other side (at a variable distance from the slots).

Initially, we calculated the normalized magnetic field value inside the 3-cell resonator at the slot position. These calculations were made by MAFIA in rz-geometry for the resonator without slots. Field values were obtained at a point on the resonator wall corresponding to the middle of the slot. Equation (9) was used for normalisation.Then, the field inside the RWG resonator was calculated by using a basic analytical model for a rectangular resonator.

The frequencies of the resonant system were found from (14). Finally, the system of equations was solved (in according with [2]):

$$\omega_i - u \tan[\psi_i + b + a(\omega_i - u)] - v = 0 \tag{15}$$

Where (ω_i, ψ_i) are the frequency-phase points and $a.b,u,v$ are the variables.

$$Q_{ext} = \frac{u}{2v} \tag{16}$$

$$\omega_0 = u$$

Figure 3 shows a very good agreement between the initial points (ω_i, ψ_i) and the calculated curve $\psi(\omega) = \operatorname{atan}\left[\frac{v}{\omega - u}\right] - b - a(\omega - u)$.

This method was tested with data for the existing 2-cell test machine and gave about the same dimensions of the slots as in the real structure.

2.3 Field inside the slot.

It is important that the surface electric field in a slot should be small in comparison with the field on a tested iris. Field on the slot surface was estimated assuming that it consists of field induced by the standing wave in the resonator and field induced by the travelling wave from the RWG. These two parts have a phase shift of 90 degrees.

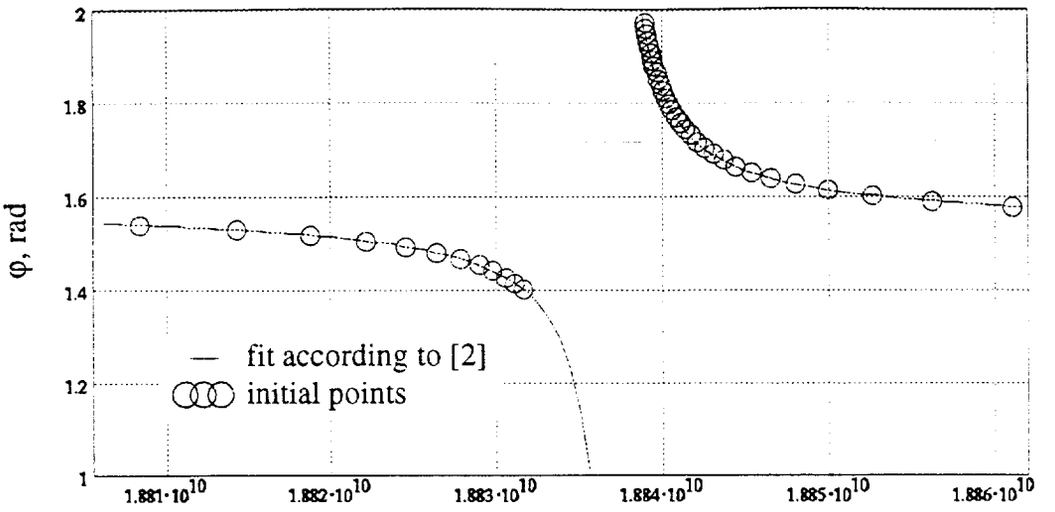

Figure 3: Curve (ω_i, ψ_i) for RWG coupled through the slots to the resonator.

The standing wave part is:

$$E1_{Smax} = \frac{Z_s(t_s, \Delta_s)\mu_0 c k^{-1} H(r_s)}{\Delta_s} \tag{17}$$

This equation was derived from equation (11) after the transformation of the voltage in the slot to the electric field strength at the middle of the slot. $H(r_s)$ is the magnetic field amplitude at the slot radius r_s in a resonator without slots, field in the RWG was set to 0 in equation (11). This field value can be calculated by MAFIA.

The travelling wave part was calculated through the integral of the Pointing's vector over the slot cross-section:

$$E2_{Smax} = \frac{P2}{Hr_s N l_s \Delta_s}\left[\frac{\tan\left(\frac{kl_s}{2}\right)}{\frac{kl_s}{2}} - 1\right]^{-1} \tag{18}$$

In these formulae: $k = \frac{\omega_0}{c}$, P is the input power.

As was shown in the calculations, the contributions from the travelling wave can be neglected, because it is about 100 times less then contribution from the standing wave.

The field strength on the iris surface and value of accelerating field were calculated by MAFIA. Results of calculations for existing 2-cell resonator (see Figure 4)and proposed 3-cell resonator are shown in Table 1. As it was found from MAFIA calculations of a standing wave resonator with slot the electric field strength on the edge of the slot can be about two times higher then the value calculated by the method described above. This effect can be avoided if the edges of the slots are rounded by some radius. By the way, in the existing device we have the slots without special smoothing. The calculated electric field strength is 35 MV/m in a slot at this power. It's not so far from such a one for 3-cells at 2 MW power, as we can see in a Table 1.

Using slots is quite interesting, because we can use slots with the same dimensions for different types of cups. Only the normalized magnetic field value at the slot position should be the

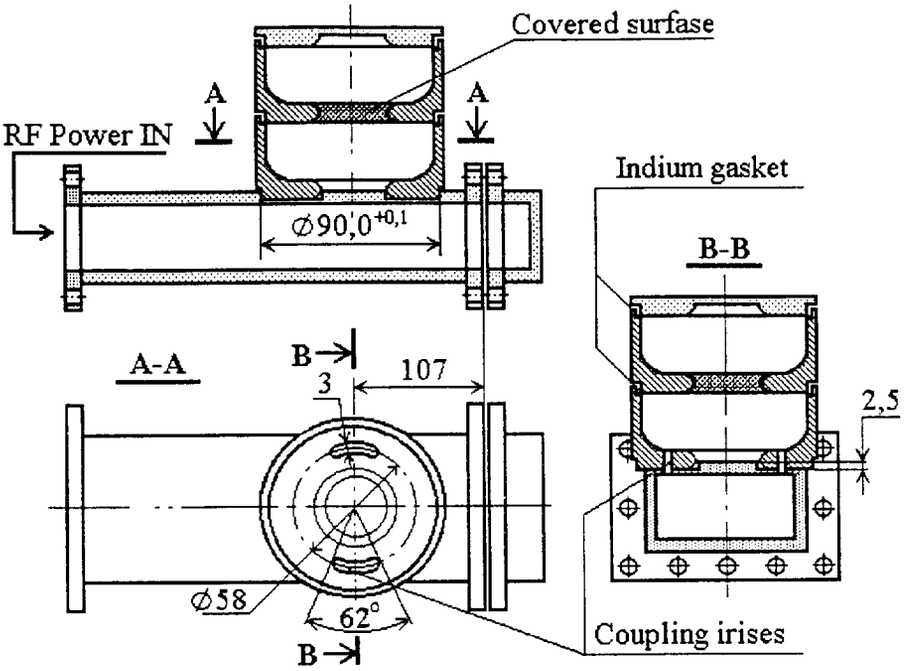

Figure 4: Construction of the 2-cells test device in according with [1]

same. On the other hand, coupling through the electric iris is very sensitive to the parameters of the cups. This variant was not accepted. The main reason to it was the cost of manufacturing.

3. Variant with coupling window.

There was another variant, which combines a conventional coupling window with the previous slot mechanism. Power comes from the RWG to the coupler through the coupling window and the coupler is connected with the resonator by means of slots.

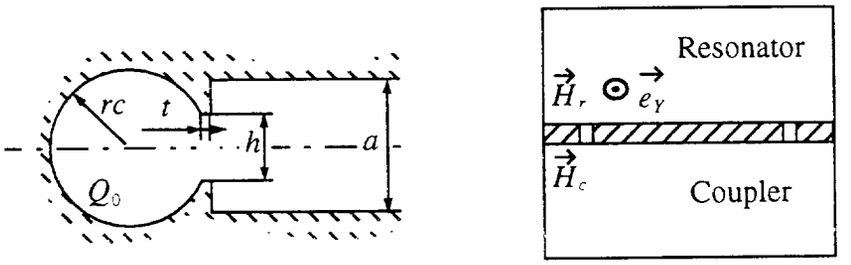

Figure 5: Main dimensions of coupling elements for variant with the coupling window

The methods for coupling window calculations for standing wave resonators are very well described in [3]. Slots effects were calculated as for the first model.

Table 1: Parameters of the existing 2-cells test machine and the proposed 3-cell test machines of Type I (coupling directly to the RWG) and Type II (coupling through the coupling cell with a window, see Chapter 3)

Type of test device	2-cell resonator. Cups with group velocity 3.7%	3-cell resonator. Cups with group velocity 3.7%		3-cell resonator. Cups with group velocity 2.2%	
	Present	Type I	Type II	Type I	Type II
Q_0	12000				
f_0, MHz	2967.3	2998.0			
t_s, mm	7	3	7	3	7
Δ_s, mm	3				
r_s, mm	29				
ϕ_s, degree	62				
Q_{ext}, calculated	11561	11344	—	11148	—
SWR	1.04	1.06	—	1.08	—
$\frac{H_\varphi(r_s)}{\sqrt{W_{stored}}}, \frac{A}{\mathrm{m}}\frac{1}{\sqrt{V \cdot A \cdot S}}$	81000	48200		48700	
E_{acc}, MV/m		40.65		42.95	
E_{iris} for test	90	90			
$E_{\text{iris}} / E_{acc}$		2.2		2.1	
required input power, MW	4	1.87		1.88	
E_{slot}, MV/m	70	46.45	26.31	48.07	27.61
$E_{Z\max}$, MV/m	73	51.29		57.27	
Parameters of coupler (see Figure 5)					
t, mm	—	—	1	—	1
h, mm	—	—	30.08	—	30.08
rc, mm	—	—	39.18	—	39.18
A	—	—	0.076	—	0.076
df_{window}, MHz			54.3		54.3

Here we show only the final formula for the input impedance of the structure from the RWG side:

$$Z_{inp} = \frac{Z_c}{Z_{\mathrm{RWG}}} = \frac{Q_0 abH_N^2\sqrt{\frac{\mu_0}{\varepsilon_0}}}{4\omega\left(1+\frac{1}{A^2}\right)\sqrt{1-\left(\frac{\pi c}{\omega a}\right)^2}}\left(\frac{\sin\frac{\pi h}{2a}}{\frac{\pi h}{2a}}\right)^2\left[4+\frac{1}{\left(\left(\frac{\omega a}{2\pi c}\right)^2-\frac{1}{4}\right)\tan^4\left(\frac{\pi(h-t)}{2a}\right)}\right]^{-1} \tag{19}$$

Here $H_N^2 = \frac{H_r}{\sqrt{W_{\mathrm{stored}}}}$ is the normalised magnetic field in a 3-cell resonator at the slot position, Q_0 is the quality factor of the resonator, a — wide RWG wall, b — narrow wall, $A = \frac{(\vec{H}_r\vec{e}_Y)}{(\vec{H}_c\vec{e}_Y)}$, h — width of the window, t — thickness of the window. Coupling cavity dimensions should be corrected with respect to the influence of the window on the resonance frequency:

$$\frac{d\omega}{\omega} = \frac{H_N^2}{1+\frac{1}{A^2}}\frac{a^2 b}{32\pi c}\sqrt{\frac{\mu_0}{\varepsilon_0}}\left(\frac{\frac{\pi h}{2a}}{\sin\frac{\pi h}{2a}}\right)^2 \operatorname{atan}\left[\left(\sqrt{\left(\frac{\omega a}{\pi c}\right)^2-1}\right)\cdot\tan^2\left(\frac{\pi(h-t)}{2a}\right)\right] \tag{20}$$

The parameters of this variant are shown in Table 1.

Disadvantages of this approach:

- complicated design (especially with vacuum envelope)
- test setup needed to find the precise coupling geometry.

4. 3-cell test resonator as a matched load for the Disk Loaded Waveguide with standard LINAC-II coupler.

A project has been adopted a project, which uses a coupler with the same dimensions, for the LINAC-II coupler. Additional cells with special dimensions should be used to match the resonator to the DLW. The main advantage is the low cost of the design part of the project, because only the matching cell dimensions need to be found and checked. Other advantages:

- the coupler geometry need not be designed;
- the matching has to be done from a $2\pi/3$ travelling wave to the standing wave of the three cell resonator, therefore only structures with a cylindrical geometry have to be computed; this reduces the numerical calculations significantly:
- a rough estimate of cell properties derived from equivalent discrete networks is possible.

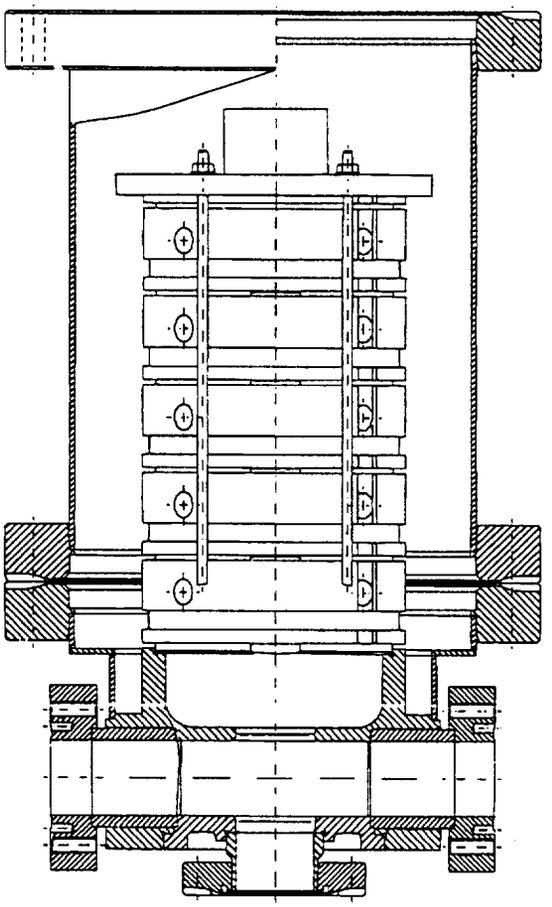

Figure 6: Proposed test device with "Linac-II" coupler.

The network model of this system was investigated to check the possibility of matching a high quality resonator to the DLW by means of one cell. This work shows, that it is possible. Next, the dimensions of this cell were found by means the MAFIA calculations. Calculations of the complete model in the travelling wave regime require a lot of CPU-time, therefore the Kroll method was used.

4.1 Application of the Kroll method to DLW.

Initially the method, described by Kroll and Yu in [2], was developed for conventional uniform waveguides. It is also applicable to disk-loaded waveguides if one takes into account a mod-

ified relationship between phase advance, length (cell number) and frequency.The phase vs frequency can be found from the dispersion curve:

$$f(\varphi) = \frac{f_{\pi/2}}{\sqrt{1 + k\cos\varphi}}$$

$$\varphi(f, N) = \mathrm{mod}\left(N\,\mathrm{acos}\left[\frac{\left(\left(\frac{f_{\pi/2}}{f} \right)^2 - 1 \right)}{k} \right], \pi \right) \tag{21}$$

$$\varphi = \begin{cases} \varphi & \varphi < \pi/2 \\ \varphi - \pi & \varphi \geq \pi/2 \end{cases}$$

In this definition k is the coupling coefficient between DLW cells, N is the number of cells between short-circuit cell and reference cell.

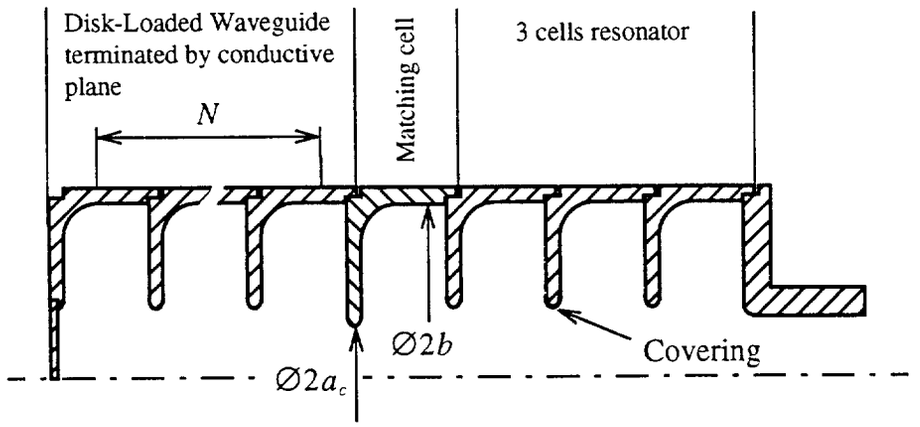

Figure 7: Resonance model of system for Kroll method calculations

4 phase-frequency points are enough to solve the system of equations (15),(16). At the $2\pi/3$ mode the resonance frequencies of the model in Figure 7 will be approximately the same with period N=3. Frequencies which correspond to N=1,2,3 were chosen. (Two $2\pi/3$ frequencies correspond to N=3.)

4.2 Network model.

The network model is shown in Figure 8. Some differences can be in definition of network parameter for each cup.

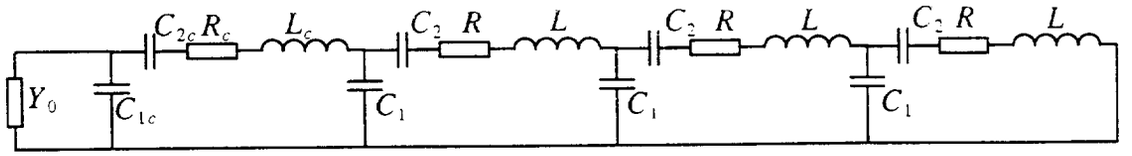

Figure 8: Network model of structure. Cells in 3-cell resonator are the same as in DLW.

The following definitions were used:

$$L = \frac{R_N \sin\varphi_0 D}{2\beta_{gr} c \tan\frac{\varphi_0}{2}}$$

$$C_1 = \frac{\tan\frac{\varphi_0}{2}}{\omega R_N} \qquad \varphi_0 = \frac{2}{3}\pi \qquad R_N = 1 \cdot \Omega \qquad \omega = 2\pi \cdot 2998 \text{ MHz} \tag{22}$$

$$C_2 = \frac{C_1}{\cos\varphi_0 - 1 + \omega^2 L C_1}$$

$$R = \frac{\omega L}{Q_0}$$

The conductivity of the DLW in the travelling wave regime:

$$Y_0 = \omega C_1 \cot\frac{\varphi_0}{2} \tag{23}$$

Two criteria were used to find the parameters of the matching cell:

1. Input conductivity of resonator with coupling cell should be equal to Y_0.
2. Imaginary part of the input impedance of DLW with matching cell should be zero from the resonator side.

We received the following data:

$$\beta_{gr} = 3.7 \qquad \text{for DLW and for the test cells}$$

$$\frac{L_c}{L} = 0.945$$

$$\frac{C_{1c}}{C_1} = 3.934 \tag{24}$$

$$\frac{R_c}{R} = 0.945$$

From this data the group velocity for the DLW, which consists of such cups, can be estimated:

$$\beta_{gr} = \frac{D \sin\varphi_0}{2\omega c C_{1c} L_c} \approx 1\% \tag{25}$$

Then, the Kroll method was tested with this data. The resonance frequencies were calculated in a model with N cells of the DLW + matching cell + 3 test cells, for the some value of Q_0. Solving the equations (15) gave the same value of Q_{ext} and f_0 with a relative error of $6 \cdot 10^{-4}$.

Correspondence between calculated curve and initial points is shown on Figure 9. On the picture Figure 10, the resonance curves for the model with different numbers of DLW cells are given.

4.3 Fields and input power

Estimations were made of the field strength in a coupling cell and the required input power. This was done by means MAFIA calculations for the case of group velocity 3.8% for the test cup. A resonance model consisting of 3 test cells, a coupling cell, and one DLW cell was used.

The following data were found for $Q_0 = 12000$ and $E_{\text{test iris}} = 90$ MV/m:

- required input power: 2.42 MW;
- surface field strength on the coupling cell iris: 40.5 MV/m;

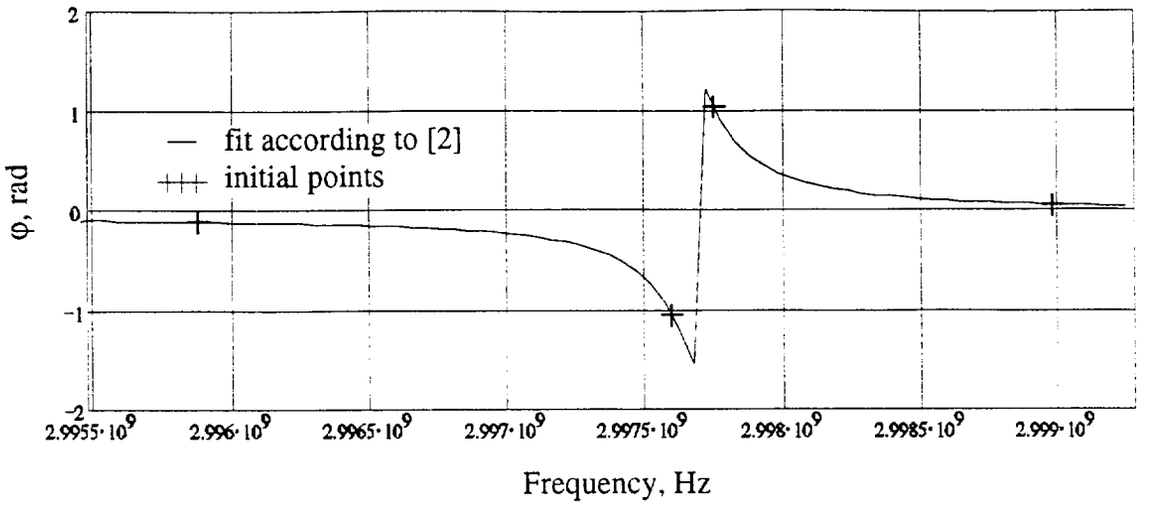

Figure 9: Application of the Kroll method to DLW

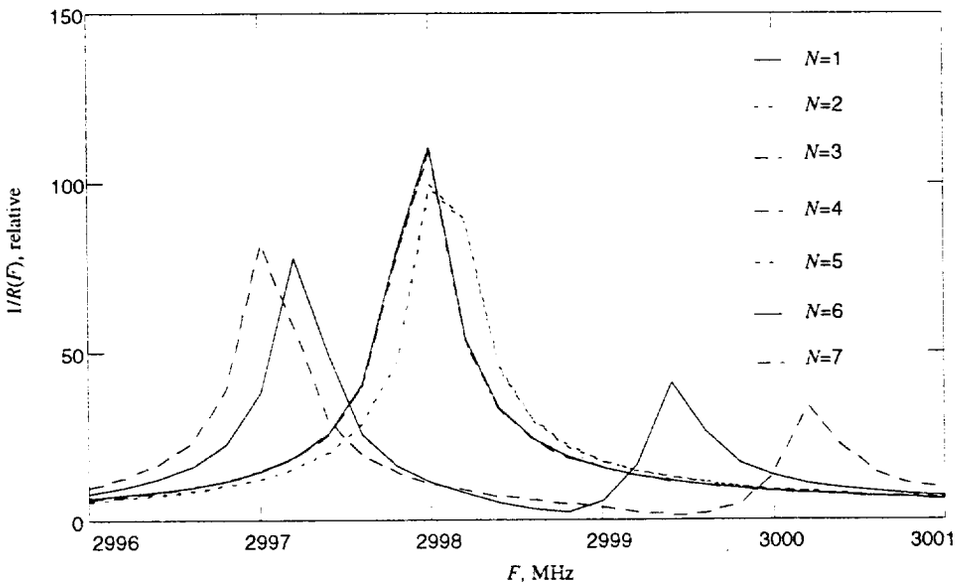

Figure 10: Resonance curves of model with different number of cells in DLW part (see Figure 7).

This variant requires some more power than the previous ones, but one can suppose that there will be no trouble with pick surface fields in the coupling elements.

4.4 Dimensions

The dimensions of the matching cell were found as a result of MAFIA calculations with the model described above. The dimensions of the SBLC-type cup with a group velocity of 1.3% were chosen as a starting point for the optimization. External quality and resonance frequency of the complete model were calculated by the Kroll method as it was shown for the network model. Calculations were made in assuming that the quality factor of the structure is about 12000. The dimensions for the manufacturing proposal are listed in Figure 11. Due to the limited numerical accuracy of the MAFIA calculations it is proposed to manufacture a set of these matching cells (with slightly different dimensions) for each type of cell.

Cups for 3-cells test machine

a, mm	b, mm	β_{gr}
11.4	39.96	0.038
11.3	39.95	
11.2	39.95	
10.8	39.94	0.037
11.0	39.95	
11.2	39.95	
10.8	39.85	0.022
10.6	39.84	
10.4	39.83	

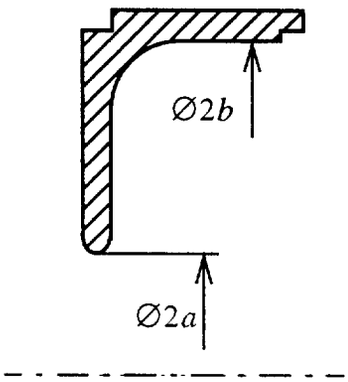

Figure 11: Proposal for the manufacturing of matching cups for three types of test cups

5. Cut-off pipe.

The new test machine needs a cut-off pipe at the short-circuit plate of the 3-cell resonator. It will be used for:

- relief of vacuum pumping of envelope volume;
- carrying out perturbation field measurements in the structure before closing the envelop.

Ø2*R*, mm	β_{gr}
19.6	0.037, 0.038
15.2	0.022

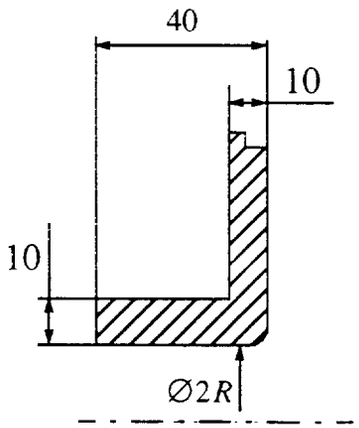

Figure 12: Cut-off pipe dimensions for two types of test cups

A pipe can be constructed with diameter which will not change the resonant frequency of the last cup. Diameters for two types of test cups were calculated by MAFIA and are presented on Figure 12.

6. References

[1] M.Dohlus et al., "High-Power Test of the Iris Coating in the S-Band Linear Collider", Internal Report DESY M 96-19

[2] N. M. Kroll, D. U. L. Yu, "Computer Determination of the external Q and resonant frequency of waveguide loaded cavities", Particle Accelerators, 1990, Vol. 34, pp. 231-250.

[3] N.Sobenin, B.Zverev, "Electrodynamic Characteristics of Accelerating Resonators", Moscow, Energoatomizdat, 220 pages, 1993

[4] V.Kaljuzhny: Private communications.